Int. J. Heat Mass Transfer. Vol. 32, No. 2, pp. 271–280, 1989
Printed in Great Britain

0017–9310/89 $3.00 + 0.00

Heat transfer from a staggered tube bundle in cross-flow at high Reynolds numbers

E. ACHENBACH
Institut für Reaktorbauelemente, Kernforschungsanlage Jülich, Postfach 19 13,
Federal Republic of Germany

(*Received* 8 *October* 1987 *and in final form* 11 *March* 1988)

Abstract—Pressure drop, integral and local heat transfer from smooth and rough staggered heat exchangers having a transverse pitch of $a = 2.0$ and a longitudinal pitch of $b = 1.4$ are measured. The range of Reynolds numbers varies from 5×10^4 to 7×10^6. Pressurized air at a pressure of up to 40 bar is used as coolant. The maximum roughness parameter applied is $k/d = 9.0 \times 10^{-3}$. The local heat transfer results are evaluated to determine the locations of boundary layer separation and transition to turbulence. Furthermore, the entrance effect on heat transfer is considered.

1. INTRODUCTION

THE PRESENT work on heat transfer from a staggered tube bundle in cross-flow is based on the preceding research on the phenomena of boundary layer flow past heat exchanger tubes [1, 2]. The heat transfer results, integral and local, complete the flow investigations and contribute to the understanding of what occurs in the boundary layer. For instance, the transition from a laminar to a turbulent boundary layer can sometimes be more easily identified from the distribution of the local heat transfer coefficient than of the skin friction.

The present investigation is concerned with heat transfer from only one tube-bundle geometry. Furthermore, the maximum Reynolds number is higher than that occurring in most technical applications. Therefore, it is not the aim of this paper to contribute to the stock of design data. However, an attempt is made to point out some fundamentals of the flow and heat transfer from tube bundles in cross-flow. Thus it will be demonstrated that the flow mechanism observed in a tube bundle is rather similar to that of a single cylinder in cross-flow. In spite of the high turbulence level generated by the repeated separation processes of the flow the boundary layer is still laminar up to high Reynolds numbers. Its transition from laminar to turbulent flow is affected by the surface roughness parameter as this was observed for the single cylinder [3]. The extension of the experiments to very high Reynolds numbers allows one to consider the transition from subcritical to transcritical flow. Thus unexpected experimental results obtained for the Reynolds number range $5 \times 10^4 < Re < 10^6$ may be explained when the effects occurring near the critical Reynolds number are known.

As mentioned above the influence of different tube arrangements on the flow and heat transfer is not treated in this paper though the geometry is an important parameter, particularly at narrow pitches of the tubes. The fundamental phenomena, however, are permanent and may help to understand the experimental evidence.

There are only a few papers about heat exchangers in cross-flow operating at very high Reynolds numbers. The most comprehensive work originated from the Kaunas group (U.S.S.R.). They tested numerous heat exchangers of different arrangements in the range $10^2 \leqslant Re \leqslant 1.5 \times 10^6$ varying the Prandtl number from 0.71 to 10^4. The results are résuméed in a book by Žukauskas *et al.* [4] published in 1968 and in Chapters 11 and 12 of a more recent volume from 1982 [5].

In 1967 Hammeke *et al.* [6] published results of a staggered and an in-line arrangement. The transverse pitch ratio of the bundle was $a = 2$, the longitudinal $b = 1.4$. The maximum Reynolds number reached was $Re = 1.5 \times 10^6$. In 1968 a paper by Scholz [7] was published which dealt with entrance effects of heat exchangers. Niggeschmidt [8] reached Reynolds numbers up to $Re = 4 \times 10^5$ and just exceeded the critical Reynolds number. Roughness effects were considered by Groehn and Scholz [9] and Groehn [10] investigated a heat exchanger with low finned tubes up to $Re = 10^6$. His results, however, are related to in-line arrangements only.

2. POTENTIAL FLOW

The potential flow through a tube bundle can be calculated by means of

$$\frac{\partial^2 \Psi}{\partial X^2} + \frac{\partial^2 \Psi}{\partial Y^2} = 0 \tag{1}$$

where Ψ is the dimensionless stream function

$$\Psi = \frac{\psi}{u_s d} \tag{2}$$

NOMENCLATURE

a transverse pitch ratio of the tubes
b longitudinal pitch ratio of the tubes
c_p heat capacity
d tube diameter
k roughness height
n exponent of the Reynolds number
p static pressure
Δp pressure drop
s_t transverse pitch of the tubes
s_l longitudinal pitch of the tubes
u streamwise velocity component
U dimensionless value of u
u_s velocity in the narrowest cross-section
v velocity component normal to the main flow direction
V dimensionless value of v
w velocity component along the cylinder contour
W dimensionless value of w
x streamwise coordinate
X dimensionless value of x
y normal coordinate
Y dimensionless value of y
z number of tube rows in streamwise direction.

Greek symbols
α heat transfer coefficient
ζ pressure drop coefficient
η fluid dynamic viscosity
λ fluid thermal conductivity
ρ fluid density
φ angle of circumference measured from stagnation point
φ_s angle of boundary layer separation
φ_t angle of boundary layer transition
ψ stream function
Ψ dimensionless stream function.

Characteristic quantities
K roughness parameter, k/d
Nu Nusselt number, $\alpha d/\lambda$
P pressure coefficient, $(p_{(\varphi)}-p_0)/((\rho/2)u_s^2)$
Pr Prandtl number, $\eta c_p/\lambda$
ξ pressure drop coefficient, $\Delta p/(z(\rho/2)u_s^2)$.

and $X = x/d$ and $Y = y/d$ denote the dimensionless coordinates.

The tube diameter, d, and the velocity, u_s, in the smallest cross section between the neighbouring tubes are considered to be the characteristic quantities of the flow through heat exchangers in cross-flow. Therefore, they are used as references in the dimensionless groups.

The stream function satisfies the equation of conservation of mass

$$\frac{\partial U}{\partial X}+\frac{\partial V}{\partial Y}=0 \tag{3}$$

by writing

$$U\equiv\frac{u}{u_s}=\frac{\partial\Psi}{\partial Y},\quad V\equiv\frac{v}{u_s}=-\frac{\partial\Psi}{\partial X} \tag{4}$$

where U and V are the velocity components in the X- and Y-directions, respectively. Together with the boundary conditions (Fig. 1)

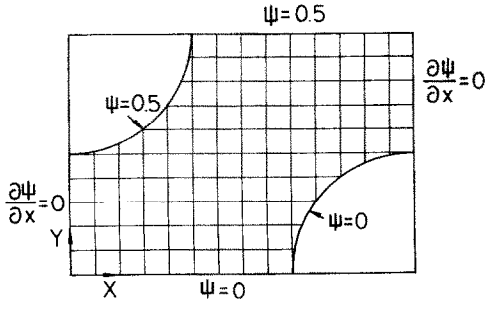

FIG. 1. Calculation domain and boundary conditions.

$\partial\Psi/\partial X = 0$ for $X = 0$ and a
$\Psi = 0$ for $Y = 0$ and along the lower cylinder contour
$\Psi = 0.5$ for $Y = b$ and along the upper cylinder contour.

Equation (1) can numerically be solved by a finite central differencing method. From the velocity distribution $W_{(\varphi)}$ along the cylinder contour where the circumferential angle, φ, is measured from the front stagnation point, the static pressure can be obtained by

$$W_{(\varphi)}^2 = U^2+V^2 \tag{5}$$

$$P_{(\varphi)} = 1-W_{(\varphi)}^2 \tag{6}$$

where $P_{(\varphi)}$ is the dimensionless pressure

$$P_{(\varphi)}=\frac{p_{(\varphi)}-p_0}{\frac{\rho}{2}u_s^2}. \tag{7}$$

Figure 2 shows the comparison of experimental and theoretical pressure distributions around the tube in the fourth row of a staggered bundle at $Re = 8\times10^6$ (present geometry: $a = 2$, $b = 1.4$). For this case and for the frontal pressure distribution of a tube in the first row ($a = b = 1.36$) as well, the theoretical and experimental results come close together (Fig. 3). Such good agreement can be expected only for the first row or for large longitudinal tube pitches. If the longitudinal pitches are so narrow that the wake flow of

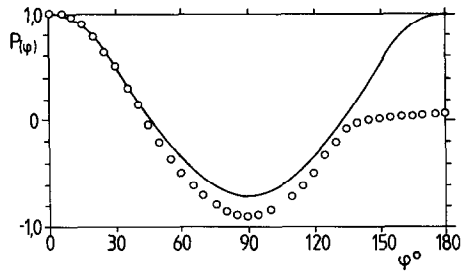

FIG. 2. Experimental and inviscid pressure distribution: $a = 2.0$, $b = 1.4$. Experiment after ref. [1], fourth row, $Re = 8 \times 10^6$.

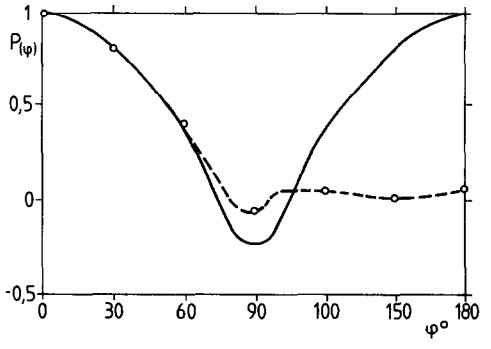

FIG. 3. Experimental and inviscid pressure distribution: $a = b = 1.36$. Experiment after ref. [11], first row, $Re = 5.6 \times 10^4$.

the preceding tube blocks the free stream area considerably, the deviations increase.

3. EXPERIMENTAL APPARATUS

The experiments have been conducted in a high pressure wind tunnel, operating with air up to 40 bar. Details of the measurement procedure for the integral and local heat transfer can be found in a previous paper [3]. Therefore, only some main data are reported here.

The test section has a cross section of 900×500 mm^2. The tube bundle consists of seven rows and three tubes per row arranged with pitch ratios of $a = 2.0$ and $b = 1.4$. The tube diameter was chosen as 150 mm.

The heat transfer measurements are performed by electrically heating only one tube of the bundle. Guard sections are provided to eliminate wall effects. The local probe has a width of 3 mm subtending an angle of circumference of $\Delta\varphi = 2.3°$. Thus a good spatial resolution is achieved for the local quantities.

The pyramidal roughness pattern of the copper test cylinder was generated by knurling. Besides the smooth surface ($k/d < 10^{-5}$) roughness parameters of $k/d = 3.0 \times 10^{-3}$ and 9.0×10^{-3} were applied. Some additional flow results for $k/d = 7.5 \times 10^{-4}$ inserted in some of the diagrams are taken from an earlier work [2].

As mentioned the surfaces of the test cylinders were manufactured by a knurling process. The remaining dummy tubes were surface-roughened by covering them with emery paper. This paper was selected in preliminary tests because the roughness types must correspond with each other [3] and must have the same effect on the magnitude of the critical Reynolds number.

4. SINGLE CYLINDER AND SINGLE ROW OF TUBES

4.1. *Single cylinder*

Heat transfer and flow past a single cylinder in cross-flow have been studied by a great number of scientists. With respect to the experimental facilities a maximum Reynolds number of $Re \approx 5 \times 10^5$ seems to be an upper threshold which cannot be exceeded without using water tunnels or pressurized gases. The latter technique has been applied for the present tests and for the preliminary investigations on the single cylinder in cross-flow as well. In those experiments [2, 12–14] maximum Reynolds numbers were reached up to $Re = 4 \times 10^6$. Summarizing the experimental results for the single cylinder obtained in the range of Reynolds numbers $2 \times 10^4 \leqslant Re \leqslant 4 \times 10^6$ the following evidence is found.

For the smooth-surfaced cylinder four flow ranges can be distinguished: the subcritical, the critical, the supercritical and the transcritical. In the subcritical flow regime ($Re < 2 \times 10^5$) the drag coefficient is almost constant, down to $Re = 10^3$. The laminar boundary layer separates at a circumferential angle of about $\varphi = 80°$ (φ measured from the front stagnation point). The total heat transfer increases with a power of $n = 0.6$ of the Reynolds number. Whereas the local heat transfer through the laminar boundary layer increases by $Re^{0.5}$ the augmentation in the rear part depends on a higher power. Thus an overall exponent of $n \approx 0.6$ results.

Exceeding $Re = 2 \times 10^5$ where this figure varies to a certain extent with the turbulence level of the incoming flow, aspect ratio, etc., the drag coefficient c_D, suddenly drops, due to a rearward shift of the separation point. At c_D-minimum—the corresponding Reynolds number is called the critical Reynolds number—the separation point is observed at $\varphi = 140°$. The skin friction distribution [3, 12] indicates that the laminar boundary layer undergoes transition to turbulent flow after laminar intermediate separation at $\varphi = 105°$. The turbulent boundary layer, however, is able to withstand the positive pressure gradient down to $\varphi = 140°$. The flow state described above is extremely sensitive to disturbances of the flow. Therefore, it is called the critical flow regime. Beyond the critical Reynolds number c_D remains on the low plateau up to $Re \approx 8 \times 10^5$.

For Reynolds numbers $Re > 8 \times 10^5$ the supercritical flow regime begins extending up to about $Re = 1.5 \times 10^6$. Immediate transition from laminar to turbulent flow occurs in the rear of the cylinder. The drag coefficient increases again due to a shift

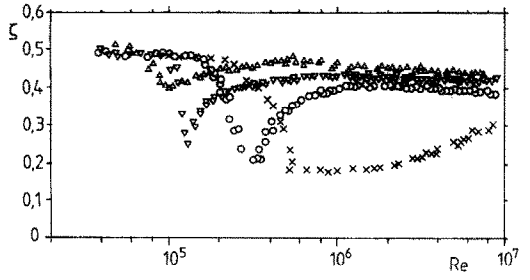

FIG. 4. Single row of tubes ($a = 2.0$); pressure drop coefficient. ×, smooth; ○, $k/d = 7.5 \times 10^{-4}$; ▽, $k/d = 3.0 \times 10^{-3}$; △, $k/d = 9.0 \times 10^{-3}$.

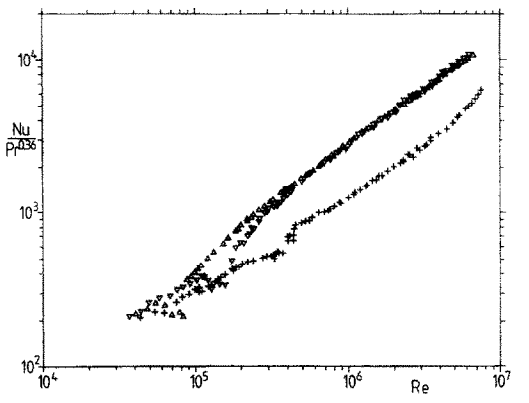

FIG. 5. Total heat transfer from a single row of tubes ($a = 2.0$). Parameter: surface roughness. Symbols as in Fig. 4.

of the boundary layer separation upstream. For $Re > 1.5 \times 10^6$ the transition point from laminar to turbulent boundary layer gradually moves towards the front stagnation point covering an increasingly larger area of the cylinder with a turbulent boundary layer. This results in a further augmentation of the heat transfer with growing Reynolds number.

For $Re > 2 \times 10^6$ the transcritical flow range is reached. Except in the vicinity of the stagnation point the boundary layer is turbulent. The separation point is fixed to about $\varphi_s = 120°$ causing a constant drag coefficient.

For the rough cylinder the experiments exhibit that the surface roughness does not change the character of the flow basically. The four flow ranges are still evident. The roughness elements predominantly affect the flow where it is most sensitive to disturbances, i.e. in the critical Reynolds number range. Therefore, an increasing roughness parameter k/d leads to lower critical Reynolds numbers due to premature onset of turbulence. This relationship is given by

$$Re_{crit} = 6000/\sqrt{(k/d)}.$$

This equation is plotted in Fig. 11 together with the results of the single row and staggered bundle. The premature transition from laminar to turbulent boundary layer causes the heat transfer to improve at lower Reynolds numbers.

4.2. *Single row of tubes*

The evidence described for the single cylinder in cross-flow is exactly the same as found for the single row of tubes. Figure 4 represents the pressure drop coefficient, ζ, vs Reynolds number which includes the surface roughness as a parameter. At subcritical flow conditions the surface roughness does not affect the pressure drop. Increasing the roughness parameter causes lower critical Reynolds numbers and an increasing pressure drop coefficient at transcritical flow.

The total heat transfer of a single row of tubes is illustrated in Fig. 5. The parameter applied is the surface roughness. It is obvious that the instantaneous occurrence of the turbulent boundary layer in the rear of the tubes at each of the critical Reynolds numbers is associated with a stepwise increase of heat transfer.

For the smooth arrangement the transcritical flow range is not yet reached at $Re = 7 \times 10^6$ since the curve shows a further increase of the slope. This is characteristic for transitional flow conditions, i.e. for the supercritical regime.

The increase of heat transfer for the two rough arrangements is nearly proportional to the Reynolds number beyond the critical Reynolds number and levels out to a slope of $n = 0.7$ at the transcritical Reynolds number. The latter flow state is reached at about $Re = 5 \times 10^5$. Realizing that at very high Reynolds numbers the boundary layers are turbulent, one would have expected a dependence of the Nusselt number on the Reynolds number exhibiting a slope of the Reynolds number of 0.75–0.8. With a view to the local heat transfer distribution (Fig. 6), however, it is obvious that the improvement of heat transfer in the separated flow region is less than in the front position of the tubes. This results in an overall slope of $n = 0.7$. For $Re > 5 \times 10^5$ the curves for the two roughnesses collapse. From this evidence it can be concluded that the improvement of the transcritical heat transfer by surface roughening has a superior

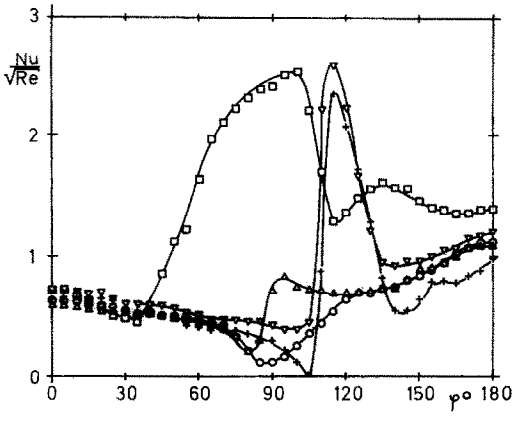

FIG. 6. Local heat transfer from a single row of smooth tubes ($a = 2.0$). ○, $Re = 1.8 \times 10^5$; △, $Re = 4.4 \times 10^5$; +, $Re = 1.2 \times 10^6$; ▽, $Re = 3.0 \times 10^6$; □, $Re = 6.9 \times 10^6$.

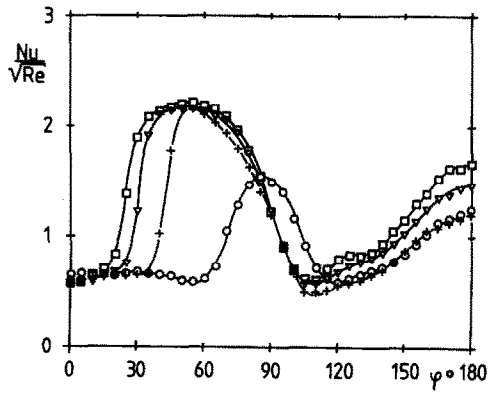

FIG. 7. Local heat transfer from a single row of rough tubes. ○, $Re = 1.8 \times 10^5$; +, $Re = 2.7 \times 10^5$; ▽, $Re = 3.4 \times 10^5$; □, $Re = 4.0 \times 10^5$.

threshold which cannot be exceeded. Similar effects occur also for the single circular cylinder in cross-flow and will be observed and discussed below for the staggered tube bundle. The critical Reynolds number, however, decreases with increasing roughness. This results in an improvement of the supercritical heat transfer already at lower Reynolds numbers.

The results for the local heat transfer distribution correspond well to the local pressure and skin friction distribution in ref. [2]. In Fig. 6 the effect of Reynolds number on the local heat transfer from a row of smooth tubes is pointed out. Experimental results are plotted for subcritical ($Re = 1.2 \times 10^6$) and supercritical flow conditions ($Re = 6.9 \times 10^6$). All curves start showing $Nu/\sqrt{Re} = 0.7$ at the stagnation point. This value tends to around unity, if the Reynolds number is formed with the velocity of the free cross section.

At subcritical flow conditions ($Re = 1.8 \times 10^5$) the curve shows a minimum of $\varphi = 80°$ indicating the laminar separation of the boundary layer. For $Re = 4.4 \times 10^5$ the flow is close to the critical one. The intermediate laminar separation is succeeded by a still feeble turbulent reattachment. This effect of laminar intermediate separation, followed by the formation of a separation bubble and reattachment to the wall as a turbulent boundary layer becomes evident for $Re = 1.2 \times 10^6$. The final separation is detected near

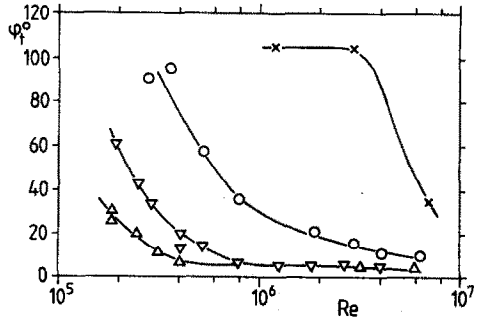

FIG. 8. Single row of tubes; transition point. ×, smooth; ○, $k/d = 7.5 \times 10^{-4}$; ▽, $k/d = 3.0 \times 10^{-3}$; △, $k/d = 9.0 \times 10^{-3}$.

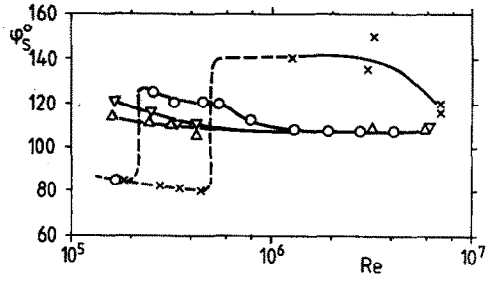

FIG. 9. Single row of tubes; separation point symbols as in Fig. 8.

$\varphi = 140°$ quite analogous to a single circular cylinder in cross-flow. For $Re = 6.9 \times 10^6$ the boundary layer undergoes transition from laminar to turbulent flow at about $\varphi = 35°$, where a sudden increase of local heat transfer is observed.

For the rough surfaced single tube row the effects mentioned above occur even at lower Reynolds numbers. It is seen from Fig. 7 that the supercritical flow regime is already reached for $Re = 1.8 \times 10^5$. Increasing the Reynolds number by a factor of two causes the transition point to move to $\varphi = 20°$.

The evaluation of the local heat transfer distributions yields data for the location of the transition and separation of the boundary layer. The position of transition from laminar to turbulent flow is plotted in Fig. 8, that of separation in Fig. 9.

Figure 8 significantly illustrates how the transition point shifts upstream with increasing Reynolds number, and that with increasing roughness parameter this effect is already observed at lower Reynolds numbers. The coarsest roughness, for instance, causes transcritical flow conditions in the entire domain of investigation as the position of transition lies immediately near the front stagnation point.

The spontaneous occurrence of the turbulent boundary layer in the rear of the tube at the critical Reynolds number is associated with a sudden displacement of the separation point downstream. This effect can impressively be recognized from Fig. 9, which shows a step in the curve at each particular critical Reynolds number.

5. STAGGERED BUNDLE

5.1. *Pressure drop*

Concerning the flow mechanism the step from a single row of tubes to a staggered tube arrangement is again gradual only. The high turbulence intensity and the interference of neighbouring tubes with one another merely smooths the boundary layer effects observed for the single row. In fact the recent increase of the pressure drop coefficient beyond a certain value of the Reynolds number or the experimental evidence of local and total heat transfer can only be understood on the basis of the knowledge about the bluff body flow.

The pressure drop coefficient of the actually inves-

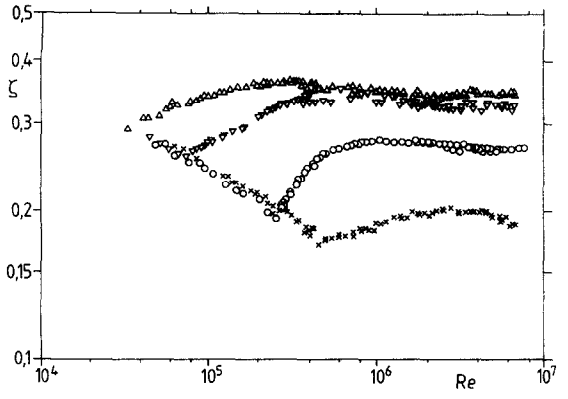

FIG. 10. Pressure drop coefficient of a staggered tube bundle ($a = 2.0$, $b = 1.4$). ×, smooth; ○, $k/d = 7.5 \times 10^{-4}$; ▽, $k/d = 3.0 \times 10^{-3}$; △, $k/d = 9.0 \times 10^{-3}$.

tigated staggered bundle is presented in Fig. 10 depending on Reynolds number and surface roughness. The critical Reynolds number for each of the particular roughness heights is indicated by the minimum of the curve. It decreases with increasing roughness parameter. The particular relationship can be correlated by

$$Re_{crit} = 3600/\sqrt{(k/d)}.$$

As shown in Fig. 11 the critical Reynolds numbers of the single row of tubes and of the whole bundle differ by a factor of two, assuming the same roughness conditions. The lower values representing the results of the bundle are due to the higher velocity of the incoming flow and the enhanced turbulence level at each tube.

While the pressure drop coefficient of the single row undergoes a steep decrease immediately before reaching the critical Reynolds number (see Fig. 4) a slight, but over a wider range falling curve is observed for the staggered bundle. With a view to the single cylinder in cross-flow at a high turbulence level where similar phenomena occur this effect may be due to the high velocity fluctuations within the tube bundle.

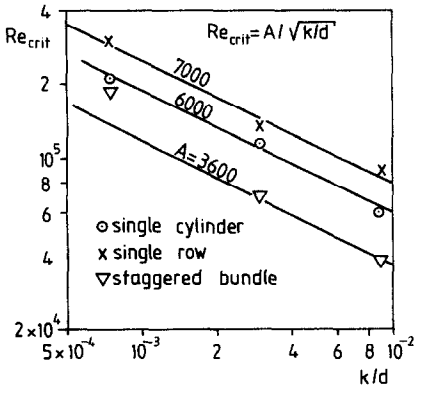

FIG. 11. Critical Reynolds number of the single cylinder, single row and staggered bundle depending on surface roughness.

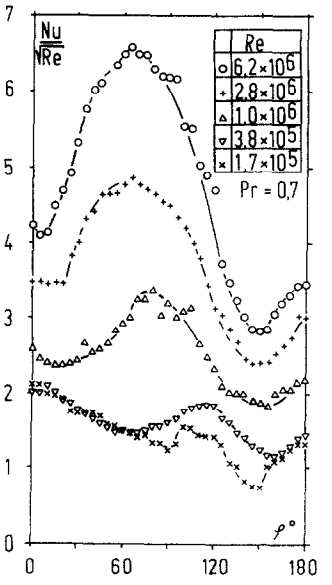

FIG. 12. Local heat transfer from a smooth staggered bundle ($a = 2.0$, $b = 1.4$). Parameter: Reynolds number.

Beyond the critical Reynolds number the pressure drop curves of the bundle are similar to those of the single row. The supercritical flow range can be recognized from the increase of the pressure drop coefficient, which then levels out to a constant value for transcritical flow conditions.

5.2. *Local heat transfer*

The experimental results of the local heat transfer coefficient are appropriate to get information about the boundary layer phenomena. Figure 12 illustrates this quantity for the smooth surfaced bundle. At $Re = 1.7 \times 10^5$ the flow is still subcritical, i.e. the boundary layer is laminar. The heat transfer coefficient decreases with increasing angle of circumference until separation occurs at $\varphi = 90°$. For $Re = 3.8 \times 10^5$ the transition to turbulent boundary layer seems to occur near $\varphi = 70°$. With increasing Reynolds number this location shifts upstream and is found for $Re = 6.2 \times 10^6$ around $\varphi = 10°$, i.e. near the front stagnation point.

Considering the local heat transfer of the staggered rough bundles (Fig. 13) it is obvious that for $Re = 1.5 \times 10^5$ the flow is already transcritical. The disturbances generated by the roughness cause the flow to undergo transition to turbulence in the immediate vicinity of the front stagnation point.

5.3. *Boundary layer separation and transition*

Whereas the transition point from laminar to turbulent boundary layer can be detected with fair accuracy from the local heat transfer distribution, the separation point is difficult to determine because of the flat minimum of the curves. Nevertheless, an attempt was made to evaluate the data.

Figure 14 illustrates the results of the boundary

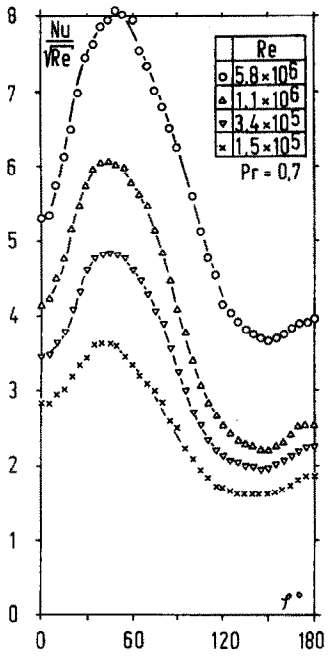

FIG. 13. Local heat transfer from a rough staggered bundle ($a = 2.0$, $b = 1.4$, $k/d = 9.0 \times 10^{-3}$). Parameter: Reynolds number.

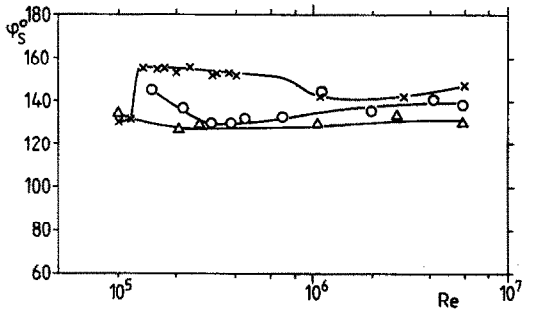

FIG. 14. Staggered tube bundle ($a = 2.0, b = 1.4$). Separation point of the boundary layer. ×, smooth; ○, $k/d = 3.0 \times 10^{-3}$; △, $k/d = 9.0 \times 10^{-3}$.

layer separation from the smooth and rough bundles. The increase of the separation angle, φ_s, at critical flow conditions is obvious for the smooth bundle only, for the results of the rough heat exchangers belong to the regime beyond the critical Reynolds number.

The position of boundary layer transition is plotted in Fig. 15 depending on Reynolds number and surface

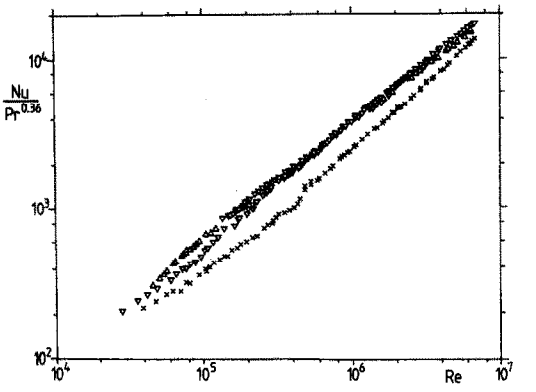

FIG. 16. Total heat transfer from a staggered tube bundle ($a = 2.0$, $b = 1.4$). ×, smooth; ▽, $k/d = 3.0 \times 10^{-3}$; △, $k/d = 9.0 \times 10^{-3}$.

roughness. Whereas for the smooth bundle the upstream shift of φ_t with increasing Reynolds number is evident, the flow is already transcritical for the rough bundles at the lower Reynolds number investigated ($Re > 2 \times 10^5$). The dashed lines indicate the probable course of the curves.

5.4. *Integral heat transfer*

The total heat transfer represents the integral of the just described local flow and heat transfer events. This quantity only exhibits remarkable evidence when all local effects are in the same direction of favouring or hindering the heat transfer. This is, for instance, the case during transition from the laminar to turbulent boundary layer. The resulting improvement of the heat transfer causes an increasing slope of the curve $Nu = f(Re)$.

Figure 16 illustrates the overall Nusselt number as a function of the Reynolds number and the surface roughness. It is obvious that surface roughening yields an essential improvement of the heat transfer beyond the critical Reynolds number. This improvement results from the occurrence of two phenomena: the first is recognized as transition to the turbulent boundary layer, the second as an extension of the turbulent boundary layer length due to the upstream shifting of the transition point with increasing Reynolds number. Both effects start at each particular critical Reynolds number for the different roughness parameters.

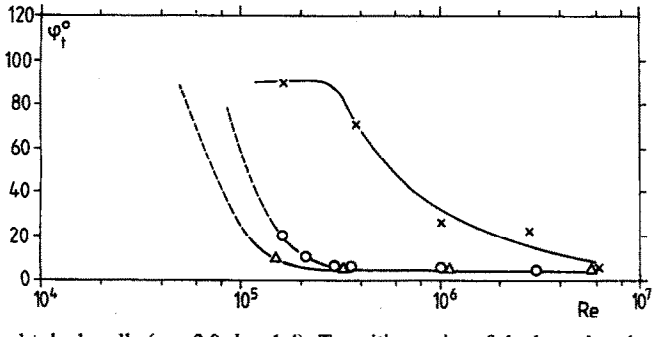

FIG. 15. Staggered tube bundle ($a = 2.0$, $b = 1.4$). Transition point of the boundary layer. Symbols as in Fig. 14.

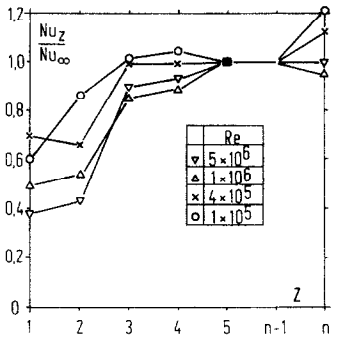

FIG. 17. Entrance effects on heat transfer for a staggered smooth bundle. n is the pointer of the tube row.

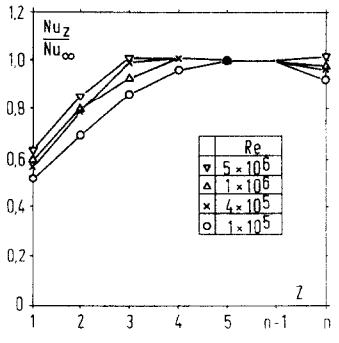

FIG. 18. Entrance effects on heat transfer for a staggered rough bundle ($k/d = 9.0 \times 10^{-3}$).

At transcritical flow conditions the results for the two rough heat exchangers collapse. The reason seems to be that both roughnesses are much higher than the boundary layer thickness. Thus variations of the roughness height have no significant effect on the boundary layer unless the roughness elements become so small that they submerge into the boundary layer. A similar effect has already been mentioned in context with the heat transfer from a single row. So it is important to know that the enhancement of transcritical heat transfer for staggered heat exchangers is not possible beyond the upper threshold given in Fig. 16 only by increasing the roughness height. Advantages from roughening can then be drawn only in the critical and supercritical flow regimes because the critical Reynolds number decreases and heat transfer improvements occur at already lower Reynolds numbers.

5.5. *Entrance effects*

It is well known that the tubes in the entrance section of a heat exchanger show lower heat transfer coefficients than tubes further downstream. This entrance effect is observed to depend on the tube arrangement, the Reynolds number and the surface roughness. As a good estimate, however, the heat transfer from the first row is about 60% of the mean value for the whole bundle, and that of the second row is around 80% of it. If the heat exchanger operates near the critical Reynolds number considerable deviations from the above figures may occur as demonstrated already in ref. [7]. In this case the first or the first and the second rows may still work under subcritical flow conditions while the succeeding rows already undergo transition to turbulent boundary layer due to the increased turbulence level associated with a higher heat transfer.

Figures 17 and 18 show the entrance effect for a smooth and a rough heat exchanger. The parameter is the Reynolds number. For the smooth bundle (Fig. 17) the boundary layers are laminar throughout for $Re = 1 \times 10^5$. Therefore, the above-mentioned percentages of 60 and 80% are nearly relevant. At higher Reynolds numbers the first and second rows have predominantly laminar boundary layers whereas downstream turbulent boundary layers prevail. Thus the first row may contribute down to 40% compared to a row further downstream.

The results reported in Fig. 18 for the rough bundle are quite analogous to those of a smooth bundle at subcritical flow conditions. This is why the flow at the present roughness parameter $k/d = 9.0 \times 10^{-3}$ is already transcritical, even in the first row. Therefore, transition effects cannot occur and the variation of heat transfer along the bundle is less than for heat exchangers operating near the critical Reynolds number.

5.6. *Comparison with the results of other authors*

Comparison of the results of the present study with those of other authors can be done only for a few of the experiments. There is no work known to the author which treats the heat transfer from smooth or rough heat exchangers at a Reynolds number $Re > 1.5 \times 10^6$. For smooth bundles refs. [4, 6] exceeded the critical Reynolds number, while ref. [8] just reached it. Results for rough staggered bundles have not been found, except those of ref. [6], which used unmachined iron tubes which cannot be regarded as hydraulically smooth at the high Reynolds number reached. Therefore, comparison can be made only for the results of the smooth bundle in a restricted Reynolds number range.

Figure 19 shows the results of the present study

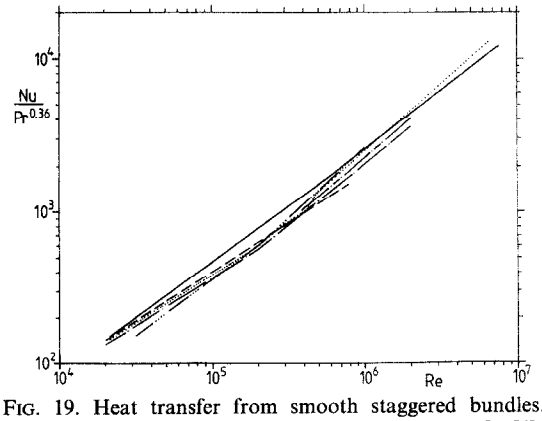

FIG. 19. Heat transfer from smooth staggered bundles. Results of different authors. ——·—·——, ref. [4]; ——·——, ref. [5]; ——···——, ref. [6]; ————, ref. [8]; ————, ref. [13]; ·····, present study.

together with those of refs. [4–6, 8, 13]. The generalized equations of refs. [4, 5, 8, 13] have been applied to the present tube arrangement and gas coolant ($Pr = 0.7$). Reference [6] used the same geometry as in this work.

For $Re < 3 \times 10^5$ all curves, except those of ref. [13] fall inside the band width of $\pm 5\%$. The result from ref. [13] lies about 10% higher than the mean value of the other ones.

For $3 \times 10^5 < Re < 1.5 \times 10^6$ the curves of the different authors split. The lowest values are predicted according to the relationships given by refs. [5, 13]. The results of the present study lie between those of refs. [4, 6] where the surface of the tubes used in ref. [6] is reported in ref. [9] to have a roughness parameter of about $k_s/d = 6.0 \times 10^{-4}$. The departures between all curves, however, are of the order of only $\pm 10\%$.

6. CONCLUSION

It has been demonstrated that the flow and heat transfer phenomena observed for a staggered tube bundle are quite similar to those known from the single cylinder in cross-flow. The existence of a critical Reynolds number indicating the transition of the laminar boundary layer to turbulence and its dependence on the surface roughness parameter are evidence of the most important fluid dynamic. The increase of heat transfer beyond the critical Reynolds number due to turbulent exchange of enthalpy across the boundary layer also illustrates that the characteristic phenomena of the bluff body flow are the prevailing features.

The experimental distribution of the local heat transfer coefficient around particular tubes of the heat exchanger reveals effects as for instance boundary layer transition or separation. It becomes evident that the transition point moves upstream with increasing Reynolds number and that with an increasing surface roughness parameter the same effect occurs already in a lower Reynolds number regime. Furthermore, the interference between the location of boundary layer separation and pressure drop becomes obvious. This exists as, according to ref. [2], the skin friction forces contribute to the total pressure drop by less than 2%, i.e. nearly the whole pressure loss is caused by shape resistance. In this sense high values of the pressure drop coefficient correspond to small angles of boundary layer separation, φ_s, and vice versa.

To demonstrate the affinity between flow and heat transfer from a single cylinder and a staggered tube bank an intermediate step was carried out via the single row of tubes. Thus the present paper also contains details for the latter geometrical arrangement.

Acknowledgements—I would like to thank my co-workers H. Gillessen, F. Hoffmanns, H. Reger and R. Rommerskirchen for their help in preparing, performing and evaluating the numerous tests.

REFERENCES

1. E. Achenbach, Investigations on the flow through a staggered tube bundle at Reynolds number up to $Re = 10^7$, *Wärme- und Stoffübertr.* **2**, 47–52 (1969).
2. E. Achenbach, Influence of surface roughness on the flow through a staggered tube bank, *Wärme- und Stoffübertr.* **4**, 120–126 (1971).
3. E. Achenbach, The effect of surface roughness on the heat transfer from a circular cylinder to the cross flow of air, *Int. J. Heat Mass Transfer* **20**, 359–369 (1977).
4. A. Žukauskas, V. Makarevičius and A. Slančiauskas, Heat transfer in banks of tubes in cross flow of fluid. *Teplofizika*, Mintis, Vilnius (1968) (in Russian).
5. A. Žukauskas, *Convective Heat Transfer*. "Nauka", Moscow (1982).
6. K. Hammeke, E. Heinecke und F. Scholz, Wärmeübergangs- und Druckverlustmessungen an querangeströmten Glattrohrbündeln, insbesondere bei hohen Reynolds-Zahlen, *Int. J. Heat Mass Transfer* **10**, 427–446 (1967).
7. F. Scholz, Einfluß der Rohrreinhenzahl auf den Druckverlust und Wärmeübergang von Rohrbündeln bei hohen Reynolds-Zahlen, *Chemie-Ingr-Tech.* **40**(20), 988–995 (1968).
8. W. Niggeschmidt, Druckverlust und Wärmeübergang bei fluchtenden, versetzten und teilversetzten querangeströmten Rohrbündeln Diss. TH Darmstadt, D17 (1975).
9. H. G. Groehn und F. Scholz, Wärme- und strömungstechnische Untersuchungen an fluchtenden Rohrbündelwärmetauschern aus pyramidenförmig aufgerauhten Rohren, Jül-Rep. 1437, July (1977).
10. H. G. Groehn, Wärme- und strömungstechnische Untersuchungen an einem querdurchströmten Rohrbündel-Wärmetauscher mit niedrig berippten Rohren bei großen Reynolds-Zahlen, Jül-Rep 1462, October (1977).
11. A. Michel, E. Heinecke und C. B. von der Decken, Messung von instationären Strömungskräften in fluchtenden und versetzten Rohrbündeln bei starren und schwingenden Rohren, Jül-Spez 2038, January (1986).
12. E. Achenbach, Influence of surface roughness on the cross-flow around a circular cylinder, *J. Fluid Mech.* **46**, 321–335 (1971).
13. *VDI-Wärmeatlas*. VDI, Düsseldorf (1984).

TRANSFERT THERMIQUE POUR UNE GRAPPE DE TUBES ETAGES EN ATTAQUE FRONTALE A NOMBRE DE REYNOLDS ELEVE

Résumé—On mesure la perte de charge, le transfert thermique local et global pour des échangeurs à tubes lisses ou rugueux étagés, avec un pas transverse $a = 2{,}0$ et un pas longitudinal $b = 1{,}4$. Le domaine de nombre de Reynolds va de 5×10^4 à 7×10^6. On utilise comme réfrigérant l'air sous des pressions allant jusqu'à 40 bar. La valeur maximale du paramètre de rugosité est $k/d = 9{,}0 \times 10^{-3}$. Les résultats de transfert thermique sont évalués pour déterminer les zones de séparation de couche limite et de transition à la turbulence. On considère aussi l'effet d'entrée sur le transfert thermique.

WÄRMEÜBERGANG EINES VERSETZTEN QUERANGESTRÖMTEN ROHRBÜNDELS BEI HOHEN REYNOLDS-ZAHLEN

Zusammenfassung—An versetzten querangeströmten glatten und rauhen Rohrbündeln des Querteilungsverhältnisses $a = 2.0$ und des Längsteilungsverhältnisses $b = 1.4$ wurden Untersuchungen zum Druckverlust sowie zum integralen und lokalen Wärmeübergang durchgeführt. Die Reynolds-Zahl wurde in den Grenzen $5 \times 10^4 \leqslant Re \leqslant 7 \times 10^6$ variiert, wobei Luft bei Drücken bis 40 bar als Strömungsmedium diente. Der Rauhigkeitsparameter betrug maximal $k/d = 9.0 \times 10^{-3}$. Die Auswertung der Ergebnisse zum lokalen Wärmeübergang lieferte Daten über die Lage der Grenzschichtablösung sowie des Umschlages laminar-turbulent. Schließlich wurde der Einlaufeffekt auf den Wärmeübergang untersucht.

ТЕПЛОПЕРЕНОС ОТ ПУЧКА ТРУБ, РАСПОЛОЖЕННЫХ В ШАХМАТНОМ ПОРЯДКЕ, В ПОПЕРЕЧНОМ ПОТОКЕ ПРИ ВЫСОКИХ ЧИСЛАХ РЕЙНОЛЬДСА

Аннотация—Измерены перепады давления, а также общий и локальный теплоперенос от гладких и шероховатых турб, расположенных в шахматном порядке, с поперечным и продольным шагами $a = 2{,}0$ и $b = 1{,}4$, соответственно. Числа Рейнольдса изменяются от 5×10^4 до 7×10^6. В качестве охладителя используется воздух под давлением до 40 бар. Максимальный параметр шероховатости составляет $k/d = 900 \times 10^{-5}$. Для определения места разделения пограничного слоя и перехода к турбулентности оцениваются результаты локального теплопереноса. Кроме того, рассматривается влияние входа на теплоперенос.